Re-entrant Negative Coulomb Drag in a 1D Quantum Circuit

D. Laroche[1,2], G. Gervais[1], M. P. Lilly[2], and J. L. Reno[2]
[1] *Department of Physics, McGill University, Montreal, H3A 2T8 CANADA and*
[2] *Center for Integrated Nanotechnologies, Sandia National Laboratories, Albuquerque, NM 87185 USA*
(Dated: June 2, 2022)

We report Coulomb drag measurements between tunable vertically-coupled quantum wires. The Coulomb drag signal is mapped out versus the number of subbands occupied in each wire, and a phase diagram for a positive versus negative drag is established. When the Coulomb drag is negative, one-dimensional subbands are observed as plateau-like features in the drag signal. Negative Coulomb drag is also observed in two regimes: one at low electronic density when the drag wire is depleted, and one at higher electronic density when the drag wire has more than a single one-dimensional subband occupied. A discussion of the negative drag signal in terms of electron-hole asymmetry and localization is presented.

PACS numbers: 73.63.Nm, 73.23.-b,

arXiv:1008.5155v2 [cond-mat.mes-hall] 1 Sep 2010

Understanding the role played by electron-electron interactions has been one of the driving forces leading to the development of coupled nanostructures designed for Coulomb drag measurements. The Coulomb drag experiment consists of coupling two independent circuits by proximity, and sending a small current I_{drive} through one of the (drive) circuits. Under the condition of no current flow, a voltage V_{drag} develops across the second (drag) circuit. This drag voltage, emanating from electron scattering between the two circuits, defines a drag resistance $R_D \equiv -V_{drag}/I_{drive}$ that is a direct probe of electron-electron interactions. The sign convention on R_D here implies that a positive (negative) drag will result from electrons in the drag circuit scattered in the same (opposite) direction than the electron flow in the drive circuit. The onset of drag voltage in a passive circuit relies on electron-hole asymmetry as charges are effectively carried both by electron-like and hole-like excitations. Without such electron-hole asymmetry, the contribution to Coulomb drag from electron-like and hole-like excitations would cancel each other, yielding no net drag signal. Recent experiments performed in quantum confined geometries such as quantum dots [1] or quantum point contacts [2] have highlighted additional contributions to transport measurements that have been attributed to a gate voltage dependent enhancement of such electron-hole asymmetry as well as to shot noise rectification, depending on the operating voltage regime [3].

Coulomb drag measurements were first performed in two-dimensional systems [4]. Subsequent studies, in agreement with the predictions from Fermi liquid theory (FL), established the drag resistivity to follow a T^2 dependence, $R_D^{2DFL} \sim \frac{T^2}{(n_1 n_2)^{3/2} d^4}$, where n_i is the electron density of each layer and d the interlayer separation. The T^2 dependence can be understood in terms of simple scattering and thermal broadening arguments as each layer contributes $k_B T$ to the drag. Accordingly, a linear temperature dependence for Coulomb drag is expected within FL theory in one dimension for identical wires [5, 6]. Within Tomonaga-Luttinger liquid theory (TLL), the situation is more complex as two competing mechanisms, backscattering [7–10] and forward scattering [11], contribute to Coulomb drag; their respective strengths depend on $2k_F d$ (k_F is the Fermi wavevector), the temperature, and the mismatch in the electron densities of each wire. A key point is that these theories predict a *positive* drag signal between two wires with negative charge carriers, *i.e.* $R_D \geq 0$. However, a negative drag signal ($R_D < 0$) was recently reported between lateral 1D-1D systems at low density [12] and heuristically attributed to Wigner crystallization in one-dimension. This experimental observation certainly demonstrates that our theoretical knowledge of Coulomb drag in one-dimensional systems is not complete.

Despite the large amount of theoretical work on the subject, very few experiments have actually measured 1D-1D Coulomb drag [12, 13]. These experiments have so far all been realized in a lateral geometry in a regime where both wires had a very similar 1D subband occupancy, where the interwire separation was large (d $\sim$ 200 nm), and where the barrier between the wires was soft (electrostatic). In order to address those limitations, we fabricated coupled quantum wires in a *vertical* geometry with the barrier grown by molecular-beam epitaxy. This design allows the mapping of the drag signal over a large range of density and subband occupancy in both wires, allowing for the precise determination of positive and negative drag regimes. Surprisingly, negative Coulomb drag is observed in two distinct regimes: one with the drag wire depleted and one with the drag wire conducting. Both of these negative drag regimes occur with the drive wire having several 1D subbands occupied. This contrasts with previous observations [12] where negative Coulomb drag was only observed when the conductance in both wires was lower than the conductance of the first plateau.

The vertically-coupled double quantum wires used in this Letter (see Fig. 1) are patterned on a n-doped

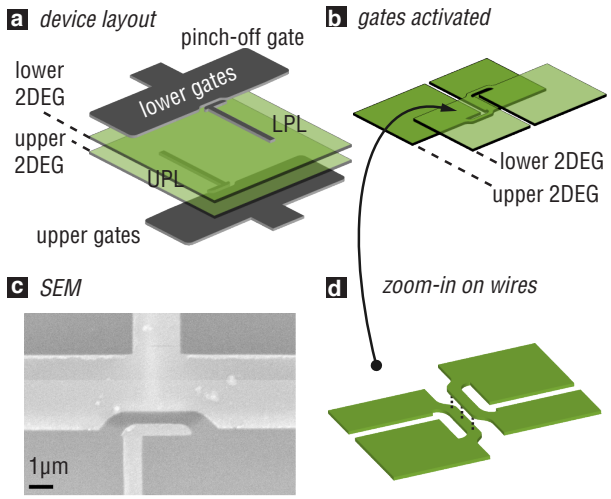


FIG. 1: (Color) **(a)** Sketch of the vertically-coupled double quantum wires device. The EBASE process causes the lower gates and the lower 2DEG to be on top of the device. **(b)** Sketch of the active part of the device when a suitable bias is applied on all four split-gates. **(c)** Scanning electron microscope picture of a similar device (here shown 2 μm long instead of 5 μm). The lower plunger (LPL) and pinch-off gates are visible on the surface of the device. **(d)** Zoom-in on the interacting region of the device.

GaAs/AlGaAs electron bilayer heterostructure (wafer EA0975). The two 18 nm wide quantum wells are separated by a 15 nm wide $Al_{0.3}Ga_{0.7}As$ barrier. The electron density is 1.1 (1.4) $\times 10^{11}$ cm^{-2} for the upper (lower) 2DEG, yielding a combined mobility of 4.0×10^5 cm^2 / V$\cdot$ s. A set of two split gates (a pinch-off gate and a plunger gate) is defined using electron beam lithography on the upper side of the sample. Using an epoxy-bound-and-stop-etch (EBASE) process [14], the sample is flipped and thinned and another set of gates is defined on the lower side of the sample. Using atomic layer deposition, a thin dielectric layer (Al_2O_3) is deposited between the lower quantum well and the lower gates to prevent electrical leakage. Due to the presence of this layer, both wires are not expected to be identically confined as the top gates are 154 nm away from the wire whereas the bottom gates are 214 nm away from the wire. The wires used are 5 μm long and 0.5 μm wide. From the alignment uncertainty, we estimate an interwire separation bounded between 33 nm and 100 nm. All transport measurements are performed at a temperature of 330 mK in a ^{3}He refrigerator. The conductance in each quantum wire is measured independently and simultaneously using two-wire measurements with an excitation voltage of 50 μV at a frequency of 9 Hz for the lower wire and 13 Hz for the upper wire. The Coulomb drag measurements are performed with a 4.5 nA current at 9 Hz, and it was verified that R_D remains the same over a large range of excitation current and frequency (0.3 - 11 nA in current and 1 Hz - 50 Hz in frequency) as well as upon inverting the drag and drive layers, provided that neither wire was depleted (*i.e.* for $G > 0.01 \times \frac{2e^2}{h}$). For the Coulomb drag results presented here, current is driven in the lower (drive) wire and voltage is measured in the upper (drag) wire.

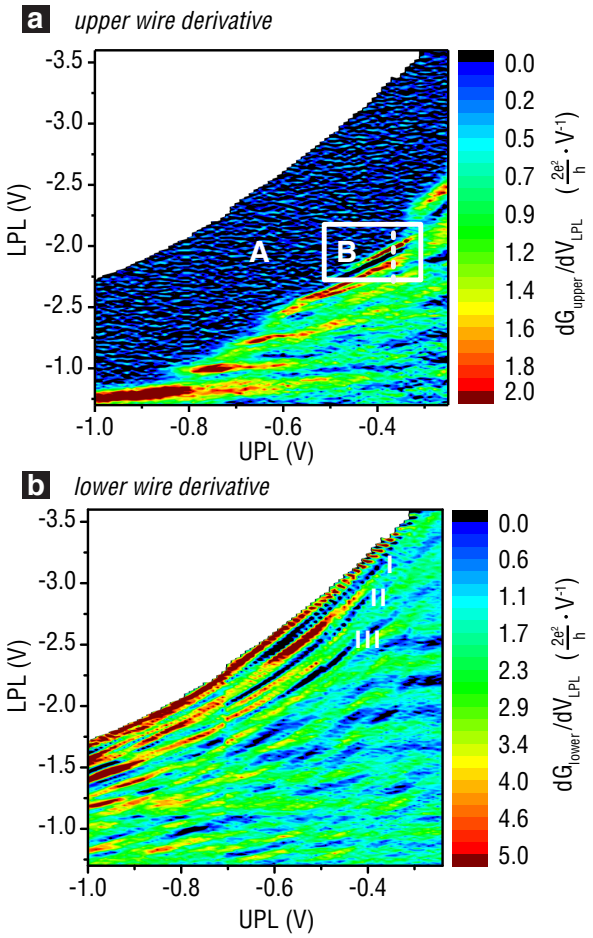


FIG. 2: (Color) **(a)** Map of the derivative of the conductance of the upper quantum wire with respect to LPL voltage. Plateau-like features appear as blue and black curves. Region **A** refers to full depletion of the upper quantum wire. Region **B** refers to the experimental region where the re-entrance of the negative drag is observed (see text). **(b)** Map of the derivative of the lower quantum wire with respect to LPL voltage.

In the Laudauer formalism, the conductance for quantum transport assumes the value $G = \frac{2e^2}{h} \sum_{i=1}^{N} T_i$ where N is the number of conduction channels and T_i is the electron transmission probability for each channel. In the ballistic regime, electron transmission is unhindered and $\sum_{i=1}^{N} T_i = N$ while an increase in scattering along the wire causes $\sum_{i=1}^{N} T_i < N$ in the non-ballistic regime. Due to their length, the wires presented in this Letter are in this non-ballistic regime and have conductance plateaus at values less than $N \times \frac{2e^2}{h}$. These plateaus can be mapped out using the plunger gates capacitively cou-

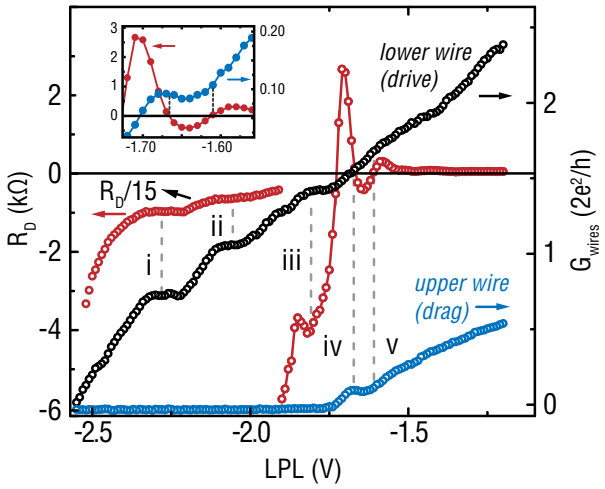


FIG. 3: (Color online) Drag resistance (left-axis) and conductance of the lower (drive) and upper (drag) wires (right-axis) as a function of the LPL voltage for fixed UPL = −0.37 V. The gray dotted lines labeled *i* through *iii* highlight conductance plateaus visible in the (low-density) negative drag signal and lines *iv* and *v* delimit the high-density negative drag regime. The high-density negative drag regime has been magnified in the inset.

pled to both wires. It is therefore possible to observe 1D subbands depopulation in each wire by sweeping a single plunger gate (*i.e.* the lower plunger gate). In addition, by varying both the upper (UPL) and the lower plunger gates (LPL), a large combination of 1D subbands is accessible and a mapping of the conductance as a function of UPL and LPL becomes possible. To highlight the position of the subbands in each wire, the numerical derivatives of the conductance with respect to the LPL voltage are presented in Fig. 2**(a)** and **(b)**. In these figures, 1D subbands can easily be identified as the derivative approaches zero for every subband crossing, appearing as blue and black stripes in the differential conductance maps, *e.g.* the dark features denoted by *I*, *II* and *III* in Fig. 2**(b)**. The wide black and blue region labeled *A* in Fig. 2**(a)** denotes the low-density regime where the upper (drag) quantum wire is depleted. The white region in the upper left corner of both figures is a non-conducting regime for both wires where data was not taken.

The drag resistance (left-axis) along with the conductance in the lower and upper wires (right-axis) is presented in Fig. 3. This data was taken during a cooldown different than the data shown in Fig. 2 and Fig. 4. The drag resistance R_D shows a strong peak at LPL = −1.71 V as the first 1D subband of the drag (upper) wire depopulates. As the upper wire density is lowered further, R_D transits towards a strongly negative regime. In this regime, subband crossings of the drive wire are clearly observed and shown in the plot by the grey lines denoted by *i*, *ii* and *iii*. We note that in the drag configuration, the tunneling resistance between the wires is ∼25 MΩ, and these features are not due to current leakage. These subband characteristics of the drive wire are however not observed in the positive drag regime. Perhaps the most striking feature of the data is the presence of a re-entrant negative drag signal occurring between LPL = −1.61 V and LPL = −1.66 V, delimited by the grey lines noted *iv* and *v* in Fig. 3, and magnified in the inset. This high-density negative drag occurs when both wires have $N \geq 1$ ($N_{drag} = 1$ and $N_{drive} = 3$). To the best of our knowledge, this is the first report of a 1D-1D negative Coulomb drag when both wires have conductance larger than that corresponding to one subband occupation.

The complete mapping (versus LPL and UPL) of the drag resistance R_D, as well as its numerical derivative dR_D/dV_{LPL}, are shown in Fig. 4**(a)** and **(b)** respectively. These maps allow the tracking of the Coulomb drag features observed in Fig. 3 over a large range of 1D subband occupancy in each wire. The strong peak observed in R_D as the first 1D subband of the drag wire depopulates occurs over the entire wires density range. It appear as stripes of negative slopes (blue) near the yellow line in Fig. 4**(b)**, but can also be observed from the darker red coloring before the drag signal becomes negative (blue) in Fig. 4**(a)**. Such peaks at the opening of a conduction channel were predicted to occur due to an enhancement of electron-hole asymmetry [3]. Plateaus in the low-density negative drag regime resulting from the drive wire 1D subband crossings can also be observed in Fig. 4**(b)** (features labeled *I*, *II* and *III* in Fig. 2**(b)** and in Fig. 4**(b)**). The transition from positive (red) to negative (blue) drag is best tracked in Fig. 4**(a)** and always occurs near the depletion point of the drag wire (yellow lines in Fig. 4). Unlike the other features mentioned previously, the high-density negative drag regime only occurs in a narrow window when UPL is between −0.33 V and −0.43 V and for LPL values corresponding to the first 1D subband crossing in the upper (drag) quantum wire. This corresponds to region *B* in Fig. 4**(a)** and **(b)**. A typical curve of this negative drag regime is shown in the inset of Fig. 4**(a)** for UPL = −0.35 V.

Previous theoretical studies of Coulomb drag in the diffusive transport regime [15] and in the non-linear regime [3] have predicted the existence of negative Coulomb drag when electrons are the sole charge carrier type. In the diffusive regime, negative Coulomb drag is expected for wires longer than the characteristic phonon assisted 1D transport length, $L_\rho = 2v_F\tau_P$, where τ_P is the phonon assisted 1D transport time. This length is estimated to be $L_\rho \sim 51$ μm [16] which is much longer than the actual wire size, 5 μm, and therefore unlikely to play a role. Likewise, it was verified that the drag voltage scales linearly with current excitation, both in the positive and negative drag regimes. Therefore, diffusive transport and non-linear drag are unlikely to explain the negative drag reported in this Letter. Negative Coulomb drag between parallel quantum wires was previously attributed

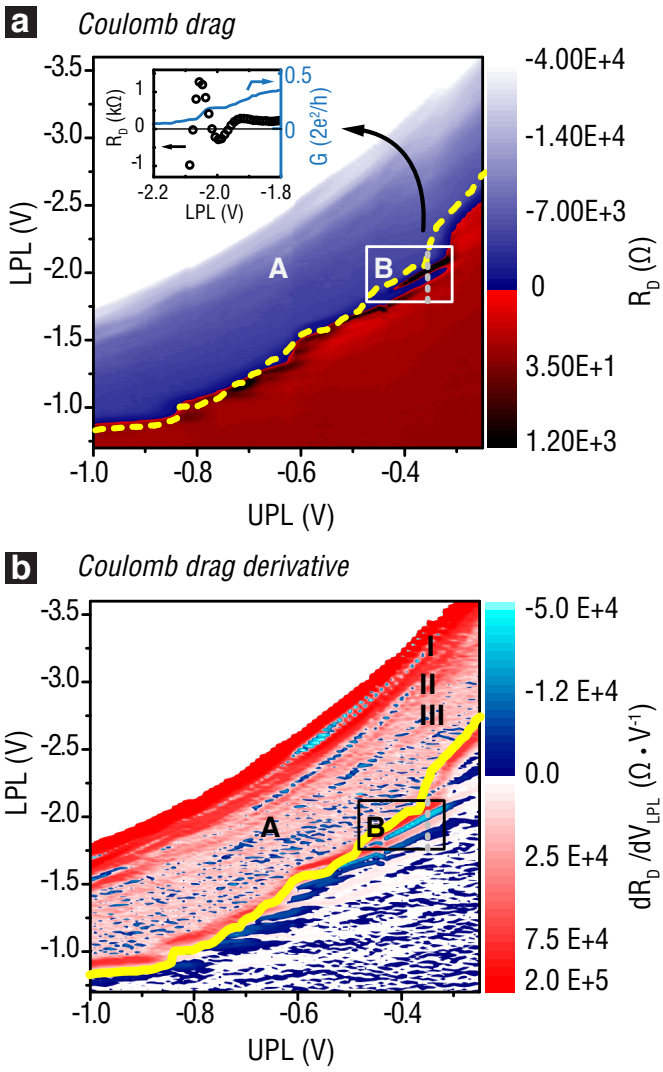


FIG. 4: (Color) **(a)** Drag resistance as a function of UPL and LPL. The color scale is set to emphasize the cross-over between positive (red) and negative (blue) drag. The yellow line delimits where the drag wire gets depleted. A trace showing the re-entrance of the negative drag is shown in the inset. **(b)** Numerical derivative of the drag resistance versus LPL gate voltage.

to Wigner crystallization [12]. While this mechanism could explain the onset of negative Coulomb drag in the low-density regime, it cannot explain the high-density negative drag observed with $N \geq 1$ in both wires. Indeed, Wigner crystallization should occur at a value of $r_s = (2na_0^*)^{-1} \geq 4$ [17], where a_0^* is the effective Bohr atomic radius. In the high-density negative drag regime, we estimate $r_s \sim 1.5$ and therefore the electrons are unlikely to form a Wigner crystal.

An enhancement of electron-hole asymmetry near the depletion of a 1D subband was predicted to cause peaks in the drag signal [3], as can be observed in our data when $N_{drag} = 1$. Compared to bulk systems, this particle-hole asymmetry is stronger in mesoscopic and quantum circuits with spatial dimension less than the temperature length $L_T = \hbar v_F/k_B T$ and the voltage length $L_V = \hbar v_F/eV$. In our Coulomb drag circuit in the high density negative drag regime, we estimate $L_T \sim 5.5\ \mu m$ at 0.33 K and $L_V \sim 1.6\ \mu m$, which are of the same order of magnitude as our quantum wire dimensions. In the linear drag regime, as is the case in this work, we expect a positive drag signal for monotonically increasing transmission probabilities, *i.e.* for monotonically increasing wire conductances. On the other hand, negative Coulomb drag might occur in the case where the conductance in the drag wire is non-monotonic. Indeed, such a non-monotonic behavior in the drag wire conductance is observed concomitant with the re-entrant negative drag (see inset of Fig. 3). We speculate that this observation might be responsible (at least in part) for the negative drag observed in the high-density regime.

To conclude, we have presented the first drag measurements between vertically-coupled quantum wires with *in situ* control over the subbands occupation of each wire. These stacked wires form quantum circuits with their own current path and gating. Our data shows a clear correlation observed between the low density negative drag and the depletion of the drag wire. While in this regime localization might explain the negative drag, the same heuristic explanation cannot explain the re-entrance of the negative drag signal observed at higher electronic density where the drag wire is conducting. We hope that this observation will motivate further theoretical work aimed at understanding the exact role played by electron interactions and electron-hole asymmetry in 1D-1D coupled electronic systems.

We acknowledge the outstanding technical assistance of Denise Tibbetts and James Hedberg. We thank Aashish Clerk for inspiring discussions. This work was performed, in part, at the Center for Integrated Nanotechnologies, a U.S. DOE, Office of Basic Energy Sciences user facility. Sandia National Laboratories is a multi-program laboratory managed and operated by Sandia Corporation, a wholly owned subsidiary of Lockheed Martin Corporation, for the U.S. Department of Energy's National Nuclear Security Administration under contract DE-AC04-94AL85000.

[1] E. Onac *et al.*, Phys. Rev. Lett. **96** 176601 (2006).
[2] V. S. Khrapai, S. Ludwig, J. P. Kotthaus, H. P. Tranitz and W. Wegscheider, Phys. Rev. Lett. **97**, 176803 (2006); **99** 096803 (2007).
[3] A. Levchenko and A. Kamenev, Phys. Rev. Lett. **101**, 216806 (2008).
[4] T. J. Gramila, J. P. Eisenstein, A. H. MacDonald, L. N. Pfeiffer and K. W. West, Phys. Rev. Lett. **66**, 1216 (1991).
[5] V. L. Gurevich *et al.*, J. Phys. Condens. Matter **10**, 2551 (1998).
[6] O. Raichev and P. Vasilopoulos, Phys. Rev. B **61**, 7511 (2000).

[7] Y. V. Nazarov and D. V. Averin, Phys. Rev. Lett. **81**, 653 (1998).
[8] R. Klesse and A. Stern, Phys. Rev. B **62**, 16912 (2000).
[9] P. Schlottmann, Phys. Rev. B **69**, 035110 (2004).
[10] G. A. Fiete, K. LeHur and L. Balents, Phys. Rev. B **73**, 165104 (2006).
[11] M. Pustilnik, E. G. Mishchenko, L. I. Glazman and A. V. Andreev, Phys. Rev. Lett. **91**, 126805 (2003).
[12] M. Yamamoto *et al.*, Science, **313**, 204 (2006).
[13] P. Debray *et al.*, J. Phys. Condens. Matter **13**, 3389 (2001).
[14] M. V. Weckwerth *et al.*, Supperlatt. Microstruct. **20**, 561 (1996).
[15] O. E. Raichev and P. Vasilopoulos, Phys. Rev. Lett. **83**, 3697 (1999).
[16] To estimate the density of the wires in the first 1D subband, we used the square root of the 2DEG density. Previous work in vertically coupled quantum wires [E. Bielejec *et al.*, Sol. State. Comm. **9573** (2008)] with similar structures have shown this to be a reasonable estimate.
[17] L. K. Saini, K. Tankeshwar and R. K. Moudgil, Phys. Rev. B **70**, 075302 (2004).